Computational Mechanics 27 (2001) 265–269 © Springer-Verlag 2001

Surface tension effects on the nonlinear behavior of long waves in a two layer flow

M. Ballas, D. Valougeorgis

Abstract The propagation of long waves of finite amplitude at the interface of two viscous fluids in the presence of interfacial tension is examined. The effect of capillarity on the shape of the waves at the interface of two superposed fluids is investigated for a wide range of density differences, viscosity ratios and imposed pressure gradients. It is found that in planar geometry surface tension stabilizes the interfacial disturbances. Attention is given to the case in which the upper fluid is more dense and comprises a thin film above the lower fluid. With the heavier fluid on the top the flow pattern is always unstable when surface tension effects are neglected. In this case the interfacial waves do not grow forever and reach a finite amplitude only when the interfacial tension is greater than a critical value.

1 Introduction

Pipeline transport of a very viscous oil is an operation that involves considerable capital investment and operating expenditure. It has been found that this cost can be significantly reduced if flow patterns, such as oil–water core-annular flows are implemented, since the addition of water as a lubricant greatly reduces the pressure drop over the pipe.

A theoretical model supplemented with experimental results was produced by Ooms et al. (1984) to study the nature of core-annular flow consisting of a very viscous oil core and water annulus through an horizontal pipe. By means of hydrodynamic lubrication theory it has been found that the wavy shape of the interface can generate pressure variations in the annular layer. These variations produce perpendicular forces on the core which counterbalance the buoyancy effect due to gravity. To simplify the mathematical modeling, the core was assumed to be solid and the interface to be a solid–liquid interface whose shape was chosen freely. The authors concluded that the appearance of a stable rippled interface is essential for the existence of such flows.

In reality the oil core has a finite viscosity and the shape of the interface is determined by the gravity and viscous forces, the pressure drop over the pipe and the interfacial tension. Therefore as a first approximation to the real flow problem, Ooms et al. (1985) calculated the finite amplitude waves for a plane Couette–Poiseuille flow of two superposed layers of fluids of different viscosity. This approximation can be regarded as realistic since the thickness of the water film, in the aforementioned core-annular flow, is very small compared to the wavelength and the pipe radius. Starting from the Navier–Stokes equations and simplifying them via perturbation analysis, they have investigated the influence of the viscosity, gravity and pressure gradients on the propagation of long finite amplitude waves neglecting surface tension effects. For the case of pure viscosity stratification with equal densities, it is concluded that the existence of such waves for any Reynolds number, already suggested by Yih (1967), is possible. It has been also found that for the case of unequal viscosities and densities, the interfacial growing waves obtained by Hooper and Boyd (1983) become stable when nonlinear effects are taken into account. All numerical results are obtained with the lower fluid being more dense compared to the upper fluid.

Hooper and Grimshaw (1985) studied the nonlinear instability at the interface between two viscous fluids. They have shown that because of surface tension and nonlinear effects, the interface can evolve to some finite amplitude steady state. Renaldy (1989) addresses the weakly nonlinear behavior of periodic disturbances in two layer flow. One of the most complete reviews of long wave and lubrication theories for core-annular flows appeared in Chen and Joseph (1991). They extend the work of Hooper and Grimshaw (1985) and compare their approach to the lubrication approximation of Papageorgiou et al. (1990).

The present study analyzes the nonlinear instability at the interface between two viscous fluids by extending the work of Ooms et al. (1985) to incorporate the influence of the surface tension. Our aim is to include this effect in the calculations for completeness of the analysis and to provide a better approximation of the oil–water core-annular flow problem by taking the lower fluid to be less dense compared to the upper fluid. This arrangement is strongly unstable and the only way to produce a finite amplitude steady state is by taking under account capillarity, which in planar geometry acts only as a stabilizing mechanism of the interfacial disturbances.

2 Analysis

The flow pattern, shown in Fig. 1, is consisting of two immiscible superposed fluids between two plates, where

M. Ballas, D. Valougeorgis (✉)
Department of Mechanical and Industrial Engineering,
University of Thessaly, 38334, Volos, Greece
e-mail: diva@uth.gr

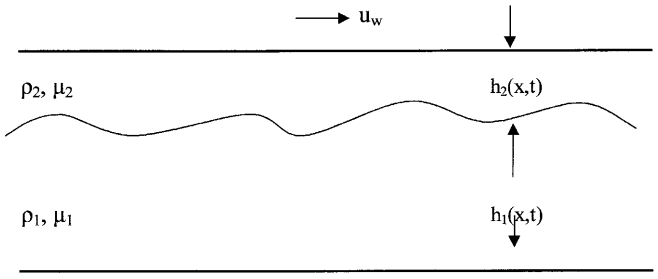

Fig. 1. Typical flow configuration

the lower plate is at rest and the upper plate is moving with velocity u_w. In this study subscripts 1 and 2 denote quantities characteristic to the lower and upper fluid respectively. The distance between the plates is h, the thickness of the two layers is $h_1(x,t)$ and $h_2(x,t)$ with $h_1 \gg h_2$, while the viscosity and density parameters are denoted by η and ρ respectively.

The analysis is restricted to two dimensional waves with a wavelength λ, large compared to the distance h between the plates $(h/\lambda \ll 1)$ and to Reynolds numbers less than or equal to one $(\rho u_w h/\eta \leq 1)$. In this case, as discussed by Ooms et al. (1985), the inertial terms are small compared to the viscous terms and the Navier–Stokes equations can be reduced to equations.

$$\frac{\partial}{\partial x}\left(h_1^3 \frac{\partial \varphi_1}{\partial x}\right) = -6\eta_1 u_i \frac{\partial h_1}{\partial x} + 6\eta_1 h_1 \frac{\partial u_i}{\partial x} + 12\eta_1 v_i \tag{1}$$

and

$$\frac{\partial}{\partial x}\left(h_2^3 \frac{\partial \varphi_2}{\partial x}\right) = -6\eta_2 (u_w - u_i) \frac{\partial h_2}{\partial x} + 6\eta_2 h_2 \frac{\partial u_i}{\partial x} + 12\eta_2 v_i \tag{2}$$

subject to the kinematics boundary condition

$$v_i = u_i \frac{\partial h_1}{\partial x} + \frac{\partial h_1}{\partial t} \tag{3}$$

and to the dynamic boundary condition

$$\varphi_1 = \varphi_2 + (\rho_1 - \rho_2) g h_1 - \gamma \frac{\partial^2 h_1}{\partial x^2} \tag{4}$$

at the interface $y = h_1$. In Eqs. (1)–(4) φ is the pressure variable, γ is the surface tension coefficient and $u_i(x,t)$ and $v_i(x,t)$ are the two components of the velocity at the interface with

$$u_i = \frac{1}{\eta_1/h_1 + \eta_2/h_2} \cdot \left(-\frac{h_1}{2}\frac{\partial \varphi_1}{\partial x} - \frac{h_2}{2}\frac{\partial \varphi_2}{\partial x} + u_w \frac{\eta_2}{h_2}\right) . \tag{5}$$

The no slip boundary conditions at $y = 0$ and $y = h$, have already been incorporated into Eqs. (1) and (2). Substituting the dimensionless quantities $H_1 = h_1/h$, $H_2 = h_2/h$, $X = x/h$, $Y = y/h$, $T = tu_w/h$, $U_i = u_i/u_w$, $V_i = v_i/u_w$, $\Phi_1 = \varphi_1 h/\eta_1 u_w$ and $\Phi_2 = \varphi_1 h/\eta_2 u_w$ into Eqs. (1)–(5) and keeping the surface tension term, the following complete set of dimensionless equations

$$\frac{\partial}{\partial X}\left(H_1^3 \frac{\partial \Phi_1}{\partial X}\right) = -6U_i \frac{\partial H_1}{\partial X} + 6H_1 \frac{\partial U_i}{\partial X} + 12V_i \tag{6}$$

$$\frac{\partial}{\partial X}\left(H_2^3 \frac{\partial \Phi_2}{\partial X}\right) = 6C_i(1 - U_i)\frac{\partial H_2}{\partial X} + 6C_1 H_2 \frac{\partial U_i}{\partial X} - 12C_1 V_i \tag{7}$$

$$V_i = U_i \frac{\partial H_1}{\partial X} + \frac{\partial H_1}{\partial T} \tag{8}$$

$$\Phi_1 = \Phi_2 + C_2 H_1 - C_4 \frac{\partial^2 H_1}{\partial x^2} \tag{9}$$

$$U_i = \frac{1}{(1/H_1 + C_1/H_2)} \cdot \left(-\frac{H_1}{2}\frac{\partial \Phi_2}{\partial X} - \frac{H_2}{2}\frac{\partial \Phi_2}{\partial X} + \frac{C_1}{H_2}\right) \tag{10}$$

and

$$H_1 + H_2 = 1 \tag{11}$$

is obtained, where $C_1 = \eta_2/\eta_1$ is the viscosity ratio, $C_2 = (\rho_1 - \rho_2) g h^2/\eta_1 u_w$ expresses the density difference, C_3 defines the dimensionless pressure drop over one wavelength and $C_4 = \gamma/\eta_1 u_w$ is the dimensionless surface tension term.

After some manipulation a single equation for the shape of the wave at the interface is obtained

$$\frac{\partial H_1}{\partial T} = \frac{\partial}{\partial X}\left[F_1\left(C_2 \frac{\partial H_1}{\partial X} - C_4 \frac{\partial^3 H_1}{\partial X^3}\right) + C_1 F_2 - \frac{C_3 + \int_{X_0}^{X_0+L}\left(\lambda_1 \frac{\partial H_1}{\partial X} - \kappa_1 \frac{\partial^3 H_1}{\partial X^3} + \mu\right) dX}{\int_{X_0}^{X_0+L} \omega_1 \, dX} \cdot F_3\right] \tag{12}$$

where

$$F_1 = \frac{(1 - H_1)^3 H_1^3}{3} \cdot \frac{1 - (1 - C_1)H_1}{(1 - C_1) \cdot \left[(1 - H_1)^4 - C_1 H_1^4\right] + C_1} \tag{13a}$$

$$F_2 = H_1^2 \frac{\left[H_1^2(1 - C_1) - 1\right](H_1 - 1)}{(1 - C_1) \cdot \left[(1 - H_1)^4 - C_1 H_1^4\right] + C_1} \tag{13b}$$

$$F_3 = \frac{H_1^2}{12} \cdot \frac{3 - 2H_1(1 - C_1)H_1^2}{(1 - C_1) \cdot \left[(1 - H_1)^4 - C_1 H_1^4\right] + C_1} \tag{13c}$$

$$\lambda_1 = C_2 \frac{1 - 4(1 - C_1)H_1 + 3(2 - 3C_1)H_1^2 - 2(2 - 3C_1)H_1^3 + (1 - C_1)H_1^4}{(1 - C_1) \cdot \left[(1 - H_1)^4 - C_1 H_1^4\right] + C_1} \tag{13d}$$

$$\mu_1 = C_1 \frac{6 - 12(1 - C_1)H_1 + 6(1 - C_1)H_1^2}{(1 - C_1) \cdot \left[(1 - H_1)^4 - C_1 H_1^4\right] + C_1} \qquad (13e)$$

$$\omega_1 = \frac{1}{2} \frac{-H_1(1 - H_1)}{(1 - C_1) \cdot \left[(1 - H_1)^4 - C_1 H_1^4\right] + C_1} \qquad (13f)$$

and

$$\kappa_1 = -\frac{C_4}{C_2} \lambda_1 \ . \qquad (13g)$$

Equation (12) may be solved for the only unknown H_1 as a function of the independent variables X and T to show the evolution of the interface, subject to an initial disturbance for the complete family of parameters under investigation. This equation reduces to Eq. (86) of Ooms et al. (1985) by assuming that the surface tension term is small compared to the pressure terms at the interface and thus $C_4 = 0$.

3 Results

The numerical results included in this section, present the departure of the wavy interface $H_1(X, T)$ from an initial sinusoidal disturbance of the form

$$H_1^{(0)} = \bar{H}_1 + A^{(0)} \sin \frac{2\pi X}{L} \ , \qquad (14)$$

where $\bar{H}_1 = 0.8$ and $A^{(0)} = 0.1$, for a wide range of parameters C_1, C_2, C_3 and C_4. For the computer simulation we have used a finite difference form of Eq. (12). A first order marching scheme in time is used, supplemented by an upwind difference for the first order spatial derivatives and central difference for all other higher order spatial derivatives. A second order McCormark scheme is also used, to provide benchmark results and to test the accuracy of the first order scheme. All the results that appear in the present work are from the first order scheme with a time step ΔT and a length step ΔX small enough to provide accurate results comparable to the McCormack scheme. In all cases enough time is given to the interface to deform and propagate.

The effect of viscosity stratification on the shape of the interface was studied first. It is clear that the present flow configuration generates a finite amplitude steady wave for all values of C_1 tested, greater or less than one. It should be noticed, that the sawtoothlike interface which exists when the less viscous liquid comprises the thin upper film and which has also been found by Ooms et al. (1985), is not developed when the more viscous liquid is at the top. Also, the equilibrium wave travels much faster when $C_1 > 1$.

The stabilizing effect of surface tension on possible instabilities due to viscosity stratification is shown clearly in Fig. 2 which presents the evolution of the interface for different values of the surface tension parameter C_4. The irregular shape of the interface for $C_1 = 10^{-4}$ ($C_2 = C_3 = C_4 = 0$) is altered dramatically even for small values of the surface tension parameter C_4. Similar behavior has been observed for the whole range of C_1 between 10^4 and 10^{-4}.

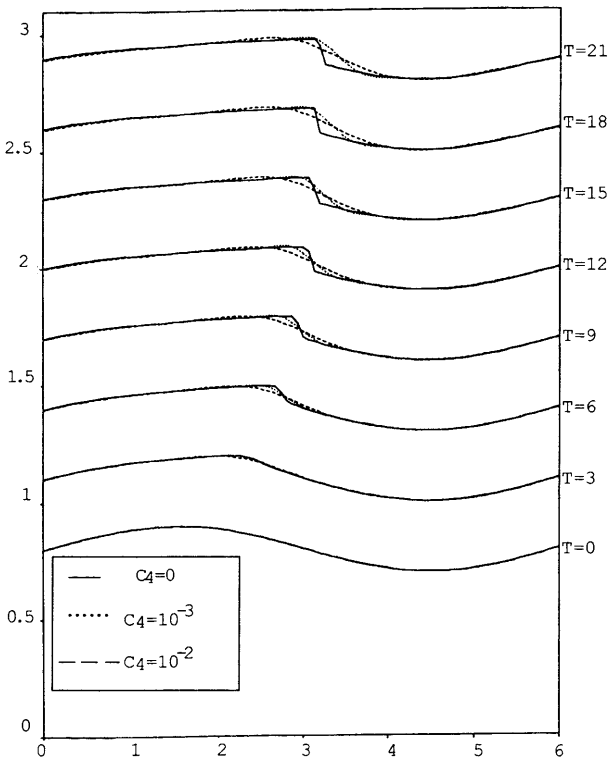

Fig. 2. Surface tension effect on the temporal evolution of an interfacial wave for $C_1 = 10^{-4}$ and $C_2 = C_3 = 0$; solutions shifted vertically by 0.3 units

The effect of capillarity is also shown for the case of the Couette–Poisseuile flow problem in Fig. 3. By setting $C_1 = 10^{-4}$ and $C_3 = -0.1$, which implies a pressure gradient opposite to the direction of movement of the upper plate, the backward facing sawtoothlike interface also produced by Ooms et al. (1985), is obtained. However, by setting $C_4 = 10^{-2}$ all regions of high interfacial curvature disappear.

Next the influence of a difference in density between the two fluids is studied, for the characteristic value of $C_1 = 10^{-4}$ and zero pressure gradient and surface tension. It is seen in Fig. 4 that for $C_2 > 0$ a damping of the wave is expected and for large values of C_2 the initial disturbance totally disappears. However, even for a small negative value of the density difference ($C_2 = -0.005$), which means that the slightly more dense fluid comprises the thin film at the top, the evolution of the wave is quite different. The wave deforms rapidly, takes an unphysical shape and the numerical solution fails. This is a clear indication that the instability derives from the deformation of the interface due to the imposed inverse density gradient. It is obvious that the instability becomes more severe for large negative values of C_2.

Finally, attention is confined in the influence of capillarity in this strongly unstable arrangement. The unstable interfacial wave observed in Fig. 4 for $C_1 = 10^{-4}$, $C_2 = -0.005$ and $C_3 = C_4 = 0$ may be stabilized if a non zero surface tension parameter is used. It is shown in Fig. 5 that for $C_4 \geq 0.02$ the amplitude of the initial disturbance does not grow with respect to time and after

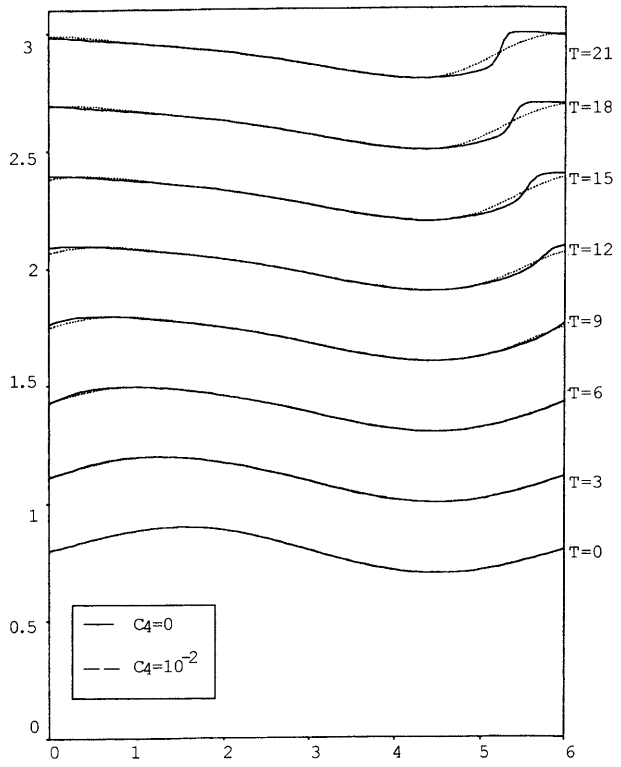

Fig. 3. Surface tension effect on the temporal evolution of an interfacial wave for $C_1 = 10^{-4}$, $C_2 = 0$ and $C_3 = -0.1$; solutions shifted vertically by 0.3 units

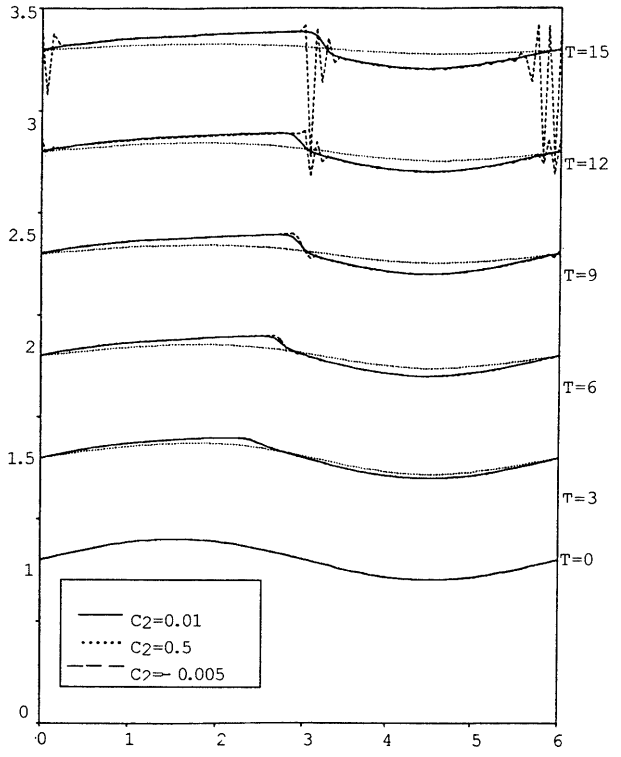

Fig. 4. Effect of density difference on the temporal evolution of an interfacial wave with a viscocity ratio of $C_1 = 10^{-4}$ and $C_2 = C_3 = 0$; solutions shifted vertically by 0.5 units

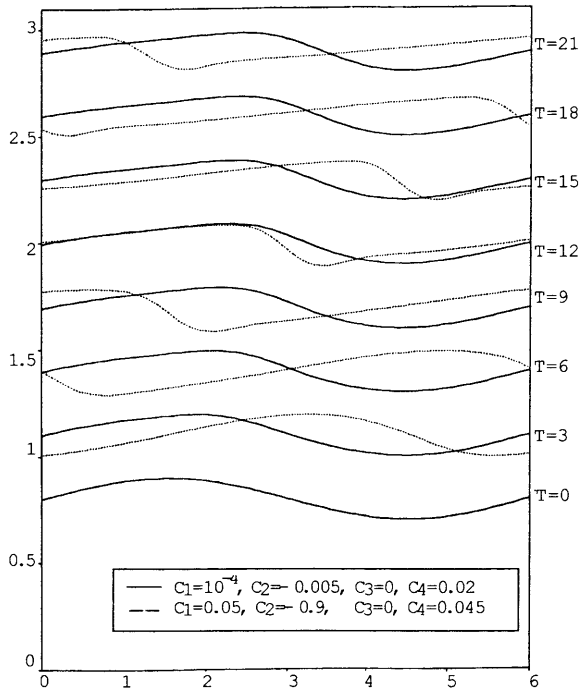

Fig. 5. Surface tension effect on the evolution of interfacial waves for negative values of C_2; solutions shifted vertically by 0.3 units

some time a wavy interface of finite amplitude is developed. Figure 5 shows also the evolution of another stable wavy interface for $C_1 = 0.05$, $C_2 = -0.9$, $C_3 = 0$ and $C_4 = 0.045$. In general when the negative value of C_2 is increased, a larger value of C_4 is required to produce stable waves. It is seen that when enough amount of capillarity is present the steepening of the forward faces of the interface profile does not result to break up. The stabilizing effect of surface tension counterbalances the destabilizing effect of negative $C_2(\rho_1 < \rho_2)$.

This is in accordance with the linear stability analysis of Babchin et al. (1983), where it is seen that when $C_2 < 0$, which implies that the heavier fluid is at the top, and $C_4 = 0$ the flow is always unstable. On the other hand, the presence of the surface tension term $C_4 > 0$ acts as a stabilizing mechanism of the Rayleigh–Taylor instability.

The implemented values of constants C_1, C_2 and C_4 correspond to characteristic sets of parameters of physical importance and have been used in the past to model experimental oil–water core-annular flow patterns.

4
Conclusions

The classical stability problem of plane Couette–Poiseuille flow of two superposed layers of fluid of different viscosity and density under the effect of surface tension has been investigated. The main flow consists of fluid 1, while fluid 2 comprises a thin lamella above fluid 1.

It has been found that by taking under account surface tension effects, Couette–Poiseuille flow is always stable when the less dense fluid comprises the thin film above the main flow. This result holds for any viscosity ratio. The flow pattern is always unstable when the more dense fluid is at the top and surface tension effects are neglected. In

this case the flow configuration becomes stable only when surface tension effects are taken under account and if the value of interfacial tension is larger than a critical value. The magnitude of interfacial tension which reduces the initial disturbance to a stable finite amplitude wave depends on the viscosity ratio, the density difference and the imposed pressure gradient.

References

Babchin AJ, Frenkel AL, Levich BG, Sivashinsky GI (1983) Nonlinear saturation of Rayleigh–Taylor instability in thin films. Phys. Fluids 26: 3159–3161

Chen KP, Joseph DD (1991) Long wave and lubrication theories for core-annular flow. Phys. Fluids A 3: 2672–2679

Hooper AP, Boyd WGC (1983) Shear-flow instability at the interface between two viscous fluids. J. Fluid Mech. 128: 507–528

Hooper AP, Grimshaw R (1985) Nonlinear instability at the interface between two viscous fluids. Phys. Fluids 28: 37–45

Ooms G, Segal A, van der Wees AJ, Meerhoff R, Oliemans RVA (1984) A theoritical model for core-annular flow of a very viscous oil core and a water annulus through a horizontal pipe. Int. J. Multiphase Flow 10: 41–60

Ooms G, Segal A, Cheung SY, Oliemans RVA (1985) Propagation of long waves of finite amplitude at the interface of two viscous fluids. Int. J. Multiphase Flow 11: 481–502

Papageorgiou DT, Maldarelli C, Rumschitzki DS (1990) Nonlinear interfacial stability of core-annular film flows. Phys. Fluids A 2: 340–352

Renaldy Y (1989) Weakly nonlinear behavior of periodic disturbances in two-layer Couette–Poiseuille flow. Phys. Fluids A 1: 10

Yih CS (1967) Instability due to viscous stratification. J. Fluid Mech. 27: 337–352